Scanning Microscopy

Volume 2 | Number 4 Article 10

8-11-1988

Transport Models for Backscattering and Transmission of Low Energy (< 3 Kilovolts) Electrons from Solids

H. Lanteri
Université de Nice

R. Bindi
Université de Nice

P. Rostaing
Université de Nice

Scanning Microscopy, Vol. 2, No. 4, 1988 (Pages 1927-1945)
Scanning Microscopy International, Chicago (AMF O'Hare), IL 60666 USA

0891-7035/88$3.00+.00

TRANSPORT MODELS FOR BACKSCATTERING AND TRANSMISSION OF LOW ENERGY (<3 KILOVOLTS) ELECTRONS FROM SOLIDS

H. Lanteri*, R. Bindi and P. Rostaing

Laboratoire d'Emission Electronique et de Luminescence
Université de Nice - Parc Valrose
06034 - NICE Cedex - France

(Received for publication April 11, 1988, and in revised form August 11, 1988)

Abstract

This paper deals with the backscattering and the transmission of electrons with energy < 3 keV through thin self supporting films, or on bulk metals.

We present the main theoretical models used in such problems, and we analyse mainly the models based on the Boltzmann transport equation, similar to those developed in our laboratory.

For any model shown here, we try to give the precise domain in which they give reliable results as well as the limitations connected to the simplifying assumptions.

In the case of the most sophisticated model, we give original results for copper. The models are presented in a comparative form, and when it is possible we compare our results with the experimental ones. The theoretical models were applied to Al and Cu. We give, for bulk metals, the values of the backscattering yield, and the energy distributions of backscattered electrons.

In the case of thin self supporting films, we studied mainly the backscattering and transmission coefficients, as well as the energy distributions of transmitted and backscattered electrons.

KEY WORDS : Backscattering and transmission of electrons through metal films, backscattered electrons, energy distributions, elastic scattering, inelastic scattering, transport equation, dielectric loss function.

*Address for correspondence:
Laboratoire d'Emission Electronique
et de Luminescence - Université de Nice
Parc Valrose - 06034 Nice Cedex - France
Phone (33) 92 52 98 98 (9657)

Introduction

Interaction of electrons with energies of some hundreds of electron volts, up to some tens of keV, with matter, is mainly constituted by elastic scattering by ions, individual or collective inelastic interactions with valence electrons, and excitation or ionization of inner shells, followed by an electronic rearrangement.

This interaction gives rise to a number of phenomena such as emission of secondary and backscattered electrons, X-ray emission and Auger effect ; Auger and X-ray emission are competing and are a result of reorganisation of the ionized atom. These phenomena are the starting points of many methods of analysis based on the electron bombardment of a target, which have been extensively developed during the last few years. Among the methods of analysis, one can mention transmission electron microscopy, scanning microscopy, microdosimetry, Auger spectroscopy, etc.

Thus, one can explain the interest in the knowledge of angular and energy distributions of electrons scattered in a material, as well as in the mechanisms of energy losses. This allows the complete characterization of the materials and the determination of yields in induced phenomena (99). For example, in electron microscopy, the knowledge of the angular distribution of electrons is necessary to estimate the image contrast. Similarly, the distribution with depth of the X-ray emission is necessary to correlate the measurements of emerging X-rays intensity to the intensity of X-rays emitted directly, the latter being itself connected to the chemical constitution of the sample (34,42,63,77). In Auger spectroscopy, the ionization of atoms by backscattered electrons gives a supplementary Auger yield, and leads to the introduction of a backscattering factor in the expression of the total Auger yield. The theoretical determination of this factor necessitates the knowledge of the angular and energy distributions of backscattered electrons in the vicinity of the surface (47,48,55,69). After a presentation of the main models for electron scattering in materials, we analyse those founded on the Boltzmann transport equation, focusing our interest, mainly on backscattering of low energy electrons (<3 keV).

The interest in such an analysis lies in the fact that for low energy electrons, the theoretical values of energy losses and mean free paths, are not easily obtained, while in the energy range over 10 keV, the theoretical computation of energy loss per unit path length founded on the Bethe-Bloch theory are in good agreement with experiment. Furthermore, as mentioned by Pouchou et al. (77) and Fitting and Reinhardt (33) low energy electrons are widely used in microanalysis, since their small depth of penetration allows the study of regions in the neighbourhood of the target surface. In the energy range 1-100 keV Neidrig (71) has analysed electron backscattering and its application to electron microscopy.

Theoretical models

According to the objective and to the energy range considered, several theoretical models of electron scattering in materials were proposed. They allow us to describe separately either the backscattering or the transmission of electrons through thin films, or both phenomena, simultaneously. These models could be classified according to different criteria : either according to the computationnal method, or to the choice of a particular parameter, such as the stopping power (energy loss by unit path length of electron), or also to the nature of the data attainable by the models. According to Adesida et al. (1) and Fathers and Rez (30), one can consider three main classes of models.

Simple models

The first concerns the models, initially developed by Everhart (29) and Archard (3). These allow us to obtain uniquely the backscattering yield as a function of the atomic number of the target. Everhart made the hypothesis that the backscattering phenomena is due to a single, large angle scattering event, while Archard assumes that electrons suffer a great number of small angle diffusions. Developments of the Everhart's model including energy distributions of backscattered electrons were proposed by Mc Afee (64), Iafrate et al. (43) and Sogard (93). A more sophisticated model was given by Kanaya and Ono (51).

Monte Carlo models

Such models are founded on the simulation of electronic trajectories and actually they are the most widely used ones. When an electron interacts with a material, its direction and its energy are modified. To simulate the electron trajectory, it is necessary to determine the trajectory length between two successive scattering events, the energy and direction of the electron after each event. These data are obtained by sampling the corresponding distributions. According to the energy of the incident electrons, and the thickness of the target, several approaches were proposed. For electrons with energies greater than some tens of keV, the multiple scattering theories are used. These allow us to determine the general result of a set of successive interactions after any step of the electron trajectory ; this method is used among others, by Patau et al. (72), Vicario and Escudie (103), and Gaber and Fitting (34).

The multiple scattering theories give correct results for energy distributions, only if the energy lost by the electron during a given path length is weak compared to its initial energy as shown by Terrissol and Patau (96). Another model, called "conventional" by Shimizu and Murata (86) is frequently used in the case of bulk samples and energies of some tens of keV. It is based on the "continuous slowing down" approximation, and uses a Bethe energy loss law, or an equivalent law (27,52,53,63). The electron trajectory is always simulated as a set of straight line segments, the residual kinetic energy at the end of an elementary path, is deduced from the energy loss law. The direction of the electron is modified according to the angular diffusion law adopted, such as Rutherford's. However, in such models, the assumption of continuous energy loss induces a fundamental defect in the energy distribution of electrons transmitted through thin films : all the electrons lose a minimum amount of energy, in contradiction with the random character of inelastic scattering. Simplified models allowing one to take into account these effects were carried out, for instance by Liljequist (60,61). The most satisfactory method for the description of electron transmission through thin self-supporting metal films, and more generally the transport of electrons with energies of about 1 keV, is the "direct simulation" method proposed among others, by Cailler and Ganachaud (18), Dejardin et al. (22), Shimizu et al. (88,89), Green and Leckey (38), Ichimura et al. (44,45), Adesida et al. (1), Akkerman and Chernov (2), Fitting and Reinhardt (33), De Salvo et al. (23,24). This model allows one to consider individually, all the scattering processes : elastic scattering, individual and collective interactions, inner-shell ionization. With this model it is sufficient to know the differential and total cross sections of the elementary processes. Clearly this model leads to more realistic electronic paths, at the expense of computing time, so, the use of this model for high energy electrons incident on bulk target is not easy.

Models based on transport equation

In this section, we group all the models founded on Boltzmann equation which was formulated initially by Bethe et al. (7) for the treatment of small angle electron scattering and neglecting the energy loss. However, in further developments (49,50) obtaining analytical solutions requires simplifying assumptions, which limit considerably the domain of validity. Numerical treatment of this equation was carried out by Brown et al. (14,15) to analyse the production of X-rays and by Bennett and Roth (6), for studies concerning secondary electron emission. The numerical methods for solving integro-differential equations avoid the use of approximations generally found in other formulations as shown by Fathers and Rez (30), Rostaing et al. (83), Lanteri et al. (56).

Theoretical models of backscattering and electron transmission based on transport equation

The models developed here are in their general behaviour similar to Monte Carlo calculations.

Continuous slowing-down model - Model I

Among the models based on the Boltzmann transport equation, it is the first and the simplest in its formulation (57,95,106). The basic assumptions are the following :

- At any time interval dt, we associate a variation ds of the electron path, $ds = |\vec{v}|dt$, where $\vec{v}$ is the electron velocity.
- A range-energy law gives for each elementary path ds, an energy loss dE. So, the inelastic processes are taken into account in the same way for all the electrons. Only, the energy loss effects are considered, the angular scattering being neglected.
- The elastic scattering is the only process contributing to angular deflection, leading to trajectories of various lengths, and then to an energy distribution of the electrons.

So, the transport equation is written :

$$\frac{1}{|\vec{v}|} \cdot \frac{\partial f}{\partial t} = \frac{\partial f}{\partial s} = - u \frac{f(s,u,x)}{\partial x} + K_e(s,u,x) \qquad (1)$$

where $f(s,u,x)$ is the density of electrons after a path length s having a velocity $\vec{v}$, a direction θ with respect to the inward normal such that $u = \cos\theta$, and located at a distance x from the surface ; $K_e(s,u,x)$ relates all the elastic processes which induce variations of the particle density per unit path length.

If we call $\sigma_e(\Theta,s)$ the differential cross section, for elastic scattering under an angle Θ ($0<\Theta<\pi$) and $\sigma_{eT}(s)$, the total cross section, the equation (1) may be written :

$$\frac{\partial f(s,u,x)}{\partial s} = - u \frac{\partial f}{\partial x} - \frac{f(s,u,x)}{\lambda_e(s)} + \frac{1}{\lambda_e(s)} \int_{-1}^{1} f(s,u',x).F_{el}(u,u')\, du' \qquad (2)$$

$$\text{with } F_{el}(u,u') = 2 \int_0^{\pi} \frac{\sigma_e(\Theta,s)}{\sigma_{eT}(s)} \cdot d\phi \qquad (3)$$

diffusion function for elastic scattering

$\lambda_e(s) = \frac{1}{n_c \sigma_{eT}(s)}$ is the elastic mean free path (m.f.p.) and n_c is the number of scattering centers per unit volume.

$u' = \cos\theta'$ is the electron direction before scattering, and ϕ the azimuthal angle.

A simplified formulation of this equation, related to the case where the small angle scattering is dominant has been widely used (7,92,94), and can be written :

$$\frac{\partial f(s,u,x)}{\partial s} = - u \frac{\partial f(s,u,x)}{\partial x} + \frac{1}{\Lambda(s)} \cdot \frac{\partial}{\partial u} \left[(1-u^2) \frac{\partial f(s,u,x)}{\partial u} \right] \qquad (4)$$

where $\Lambda(s)$ is the "transport m.f.p." defined by Bethe et al. (7)

$$\frac{1}{\Lambda(s)} = \pi \cdot n_c \int_0^{\pi} \sigma_e(\Theta,s) \cdot (1-\cos\Theta) \sin\Theta \, d\Theta \qquad (5)$$

This equation has been applied by Brown and Ogilvie (14), Bennett and Roth (6) and Lanteri et al. (56,57) to backscattering analysis, and by Rostaing et al. (82) to the transmission of electrons through thin films.

In the continuous slowing down models, whatever the choice of the cross section and of the energy-loss law, all the electrons transmitted through thin films lose a minimal amount of energy corresponding to straight line trajectory, i.e., to a path length equal to the target thickness. This anomaly prohibits the application of such models in the analysis of the transmission problems. To overcome this shortcoming we developed a model allowing one to take into account, the energetic effects in the inelastic scattering and to introduce the angular effect in such processes in a more convenient way.

Model II

This model developed by Lanteri et al. (58) takes into account the energy dispersion due to inelastic processes (straggling). The basic concept was presented in a simplified way by Birkhoff (11) and applied by Cowan and Hölzl (20) among others. In the steady state the transport equation is written :

$$0 = - \frac{\vec{p}}{m} \nabla_{\vec{r}} f(\vec{r},\vec{p}) + K_e(\vec{r},\vec{p}) + K_{in}(\vec{r},\vec{p}) \qquad (6)$$

where $f(\vec{r},\vec{p})$ is the particle density, m the particle mass, $\vec{p}$ the momentum, and $\vec{r}$ the position coordinates.

The terms $K_e(\vec{r},\vec{p})$ and $K_{in}(\vec{r},\vec{p})$ are related respectively, to the elastic and inelastic processes inducing, per unit time, a variation of the density of particles.

With fig. 1, we can write in the case of azimuthal symmetry :

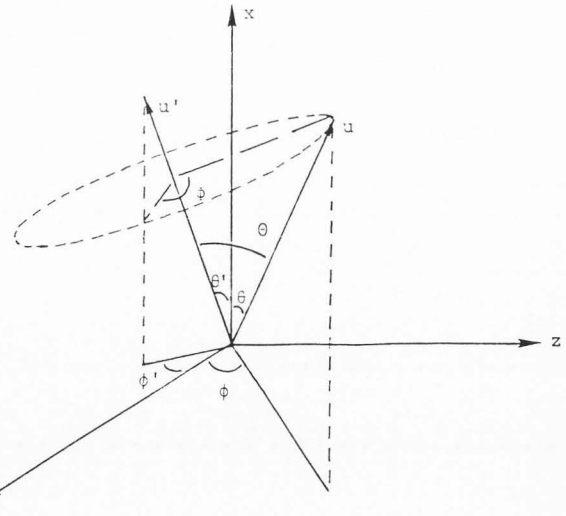

Figure 1. Geometry of our system.

$$0 = - u|\vec{v}|\frac{\partial f(E,u,x)}{\partial x} + K_e(E,u,x) + K_{in}(E,u,x) \quad (7)$$

where E is the particle energy and v,u,x as defined in "Model I".
If the full terms for K_e and K_{in} are inserted in eq. (7), one can write :

$$0 = - u\frac{\partial f(E,u,x)}{\partial x} - \frac{f(E,u,x)}{\lambda_e(E)} \quad (8)$$
$$+ \frac{1}{\lambda_e(E)}\int_{-1}^{1} f(E,u',x)\, F_{el}(u,u')\, du' - \frac{f(E,u,x)}{\lambda_{inT}(E)}$$
$$+ \int_{\Omega}\int_{E}^{E_o} \frac{|\vec{v}'|}{|\vec{v}|}\frac{1}{\lambda_{inT}(E)} f(E',u',x)\, F(E,E',\alpha)\, dE'd\Omega$$

with $F_{el}(u,u') = \int_o^{2\pi} \frac{\sigma_e(E,\ )}{\sigma_{eT}(E)}\, d\phi$

and $F(E,E',\alpha) = \frac{\sigma_{in}(E',\alpha)}{\sigma_{inT}(E')}\,\delta(E-E'\cos^2\alpha) \quad (9)$

α = inelastic scattering angle
E_o = energy of the incident electrons
$\sigma_{in}(E',\alpha)$ = inelastic differential cross section
$\sigma_{inT}(E')$ = inelastic total cross section
$\lambda_{inT}(E)$ = total inelastic m.f.p.
E' = electron energy before interaction
E = electron energy after interaction

Introducing : $\psi(E,u,x) = v.\frac{f(E,u,x)}{\lambda_T(E)} \quad (10)$

and : $\frac{1}{\lambda_T(E)} = \frac{1}{\lambda_e(E)} + \frac{1}{\lambda_{inT}(E)} \quad (11)$

the equation (8) can be written :

$$\psi(E,u,x) = -\lambda_T(E)u\frac{\partial\psi(E,u,x)}{\partial x}$$
$$+ \int_{-1}^{+1}\frac{\lambda_T(E)}{\lambda_e(E)}\psi(E,u',x)\, F_{el}(u,u')\, du' \quad (12)$$
$$+ \int_{\Omega}\int_{E}^{E_o}\frac{\lambda_T(E')}{\lambda_{inT}(E')}\psi(E',u',x)\, F(E,E',u,u')dE'\, d\Omega$$

This equation appears in the literature only in two simplified forms, each one showing only one aspect of the problem, either the elastic aspect with the corresponding equation named "Transfer equation", or "Fokker-Planck (49,50) equation" when small angle scattering is prominent, or the inelastic aspect which leads to the "energy distribution equation", and to the "straggling" phenomena (3,29,107).

Model III

This model carried out by Rostaing et al. (84) is very close in its form, to the previous one, but it allows us to make a better and much more detailed analysis of the inelastic processes, and to point out the existence of a fine structure in the electron energy spectra. Thus, in this model, the interactions with jellium and the ionisation of the inner shells are treated separately. For metals such as aluminium, the interactions with the jellium separate into individual and collective processes. So, if the errors in the numerical treatment are minimized by a convenient choice of the discretisation steps, the purely theoretical Model III allows us to check the validity of the cross sections of the physical scattering processes. In the case of noble metals, the interactions with the jellium will be considered as a whole, but they are always distinct from inner shell effects. In the particular case of copper the use of an experimental dielectric loss function is only a way to overcome the lack of theoretical information. In the transport equation the elastic scattering leads to a term in the form previously shown in Models I and II, but the cross sections will be computed by the "partial wave" method which gives more reliable values for m.f.p.'s, mainly for noble metals. The transport equation is now written in the case of N inelastic processes (83) :

$$\psi(E,u,x) = -\lambda_T(E)u\frac{\partial\psi(E,u,x)}{\partial x}$$
$$+ \int_{-1}^{+1}\frac{\lambda_T(E)}{\lambda_e(E)}\psi(E,u',x)\, F_{el}(u,u')\, du' \quad (13)$$
$$+ \sum_{i=1}^{N}\int_{\Omega}\int_{E}^{E_o}\frac{\lambda_T(E')}{\lambda_i(E')}\psi(E',u',x)\, F_i(E,E',u,u')\, dE'd\Omega'$$

The knowledge of the diffusion functions F_i of any inelastic process, leads, for the mean energy loss during an inelastic collision, to the expression :

$$\overline{\Delta E} = \int_o^{E-E_F}\Delta E\, F(\Delta E)\, d(\Delta E) \quad (14)$$

where E_F is the Fermi energy and if we denote

$$F = \sum_1^N \frac{\lambda_{inT}}{\lambda_i} F_i \quad (15)$$

we can write $$\overline{\Delta E} = \sum_{i=1}^{N}\frac{\lambda_{inT}}{\lambda_i}\overline{\Delta E}_i \quad (16)$$

where $\overline{\Delta E}_i$ is the mean energy loss for an inelastic interaction of type i. The total energy loss per unit path length is thus given by :

$$S = \sum_{i=1}^{N}\frac{\overline{\Delta E}_i}{\lambda_i} \quad (17)$$

In this formulation, the energy and angular distribution of all the inelastic processes are taken into account. The application to the analysis of the transport processes for a given metal depends only on the knowledge of the differential cross sections of the elementary processes. This model is therefore similar to the "direct Monte Carlo simulation".

Scattering cross sections

Elastic scattering - Interactions with ions

Two cross sections were considered, a Rutherford cross section with a screening parameter and a more realistic cross section computed by the "partial wave method".

Rutherford cross section : This cross section used by many authors can be written :

$$\sigma_e(E,\Theta) = \frac{Z^2e^4}{4E^2}\frac{1}{(1 - \cos\Theta + 2\xi)^2} \quad (18)$$

where ξ is a screening parameter which allows us to avoid the divergence for zero diffusion angles and maintains the strongly forward prominent character of the diffusion.

The total cross section is :

$$\sigma_{eT}(E) = \frac{Z^2 e^4}{4\,E^2} \cdot \frac{\pi}{\xi(1+\xi)} \qquad (19)$$

and the elastic m.f.p.

$$\lambda_e(E) = \frac{4AE^2}{\pi N_A \rho Z^2 e^4}\,\xi(1+\xi) \qquad (20)$$

Thus, the knowledge of m.f.p. values found in literature allows us to calculate values of $\xi(E)$ used in our computations.

The diffusion function can be written :

$$F_{el}(u,u') = \frac{2\xi(1+\xi)\,(1+2\xi - uu')}{\left[(u-u')^2 + 4\xi(1-uu') + 4\xi^2\right]^{3/2}} \qquad (21)$$

This expression written by Strickland and Bernstein (95) was generalised by Lanteri et al. (57) and used in backscattering computations (56). However, as pointed out by Krefting and Reimer (54), this cross section is only a very rough approximation, and therefore, not suitable in the case of heavy metals (44).

Cross sections given by the partial wave method

The previous cross section is mainly used in the energy range over 1 keV, but fails in the low energy range. In the partial wave method, the crystalline potential is a "muffin tin" potential, that is with a spherical symmetry inside the Augmented Plane Waves (APW) spheres, and a constant value outside the spheres. These computations were carried out by Ganachaud (35) and Mignot (68) ; the differential cross section can be written :

$$\sigma_e(E,\Theta) = \frac{1}{k^2}\left|\sum_{\ell=0}^{\infty}(2\ell+1)\,e^{i\delta_\ell}\sin\delta_\ell\,P_\ell(\cos\Theta)\right|^2 \qquad (22)$$

where E is the electron energy, Θ the elastic scattering angle, k the wave vector of the incident electron, δ_ℓ is the phase shift between the ℓ^{th} partial wave and the free spherical wave, and the P_ℓ are the Legendre polynomials. The total cross section is given by :

$$\sigma_{eT}(E) = \frac{4\pi}{k^2}\sum_{\ell=0}^{\infty}(2\ell+1)\sin^2\delta_\ell \qquad (23)$$

A comparison between these two cross sections was carried out for several metals, by Ichimura et al. (44) and by Valkealahti and Nieminen (102). The cross section given by means of partial waves expression method of Mott was largely used, namely by Kotera et al. (53) with various crystalline potentials. The values thus obtained are very close for all the potential chosen by these authors. For energies of about 1 keV, such cross sections are quite different of Rutherford screened cross section particularly for small deviations where they are higher. This result is analogous to that observed with our computations by partial waves method. Thus, the Mott cross section could also be used in our computations and will allow us to take into account in a realistic way the small angles scattering effects.

Inelastic scattering

Model I - In this model, we use either the theoretical energy-range relation given by Bethe et al. (7), or experimental laws related to maximal ranges or to practical ranges. The experimental laws are generally written in the form :

$$s = A(E_o^l - E^l(s)) \qquad (24)$$

where E(s) is the incident electron energy after a path length s, A a constant depending on the material, and $1.3 < l < 1.6$.

Model II - In this model the whole inelastic phenomena are taken into account by means of a Rutherford cross section :

$$\sigma_{inT}(E,\alpha) = \frac{n_e^4}{E^2} \cdot \frac{\cos\alpha}{\sin\alpha} \qquad (25)$$

Zeller and Ruste (107), Dashen (21) and Lanteri et al. (58) introduced a minimum scattering angle "α_m" given, in non relativistic kinematics and under the assumption of the target electron at rest, by :

$$\alpha_m = \arcsin\left(\frac{\Delta E}{E}\right)^{1/2} \# \left(\frac{\Delta E}{E}\right)^{1/2} \qquad (25bis)$$

where ΔE is the energy loss, and E, the electron energy. This will avoid divergences for zero scattering angle and leads to a minimum energy loss in an inelastic scattering event :

$$\Delta E = E \sin^2\alpha_m$$

the inelastic m.f.p. is then given by :

$$\lambda_{inT}(E) = \frac{AE^2}{N_A \rho Z \pi e^4 \,\mathrm{tg}^2\alpha_m} \qquad (26)$$

and the mean energy loss by unit path length will be :

$$\overline{\Delta E} = -\frac{2N_A \rho Z \pi e^4 \,\mathrm{Log}\sin\alpha_m}{A.E} \qquad (27)$$

Thus, the parameter "α_m" could be computed either according to the values of the m.f.p. found in the literature, or, according to experimental or theoretical values of the energy loss per unit path length.

Then, the diffusion function for inelastic scattering can be written :

$$F(E,E',\alpha) = \frac{\mathrm{tg}^2\alpha_m}{\pi}\,\frac{\cos\alpha}{\sin^4\alpha}\,\delta(E-E'\cos^2\alpha) \qquad (28)$$

Taking into account the angular relation :

$$u' = u\left(\frac{E}{E'}\right)^{1/2} - \left[(1-u^2)\left(1-\frac{E}{E'}\right)\right]^{1/2}\cos\phi \qquad (29)$$

where ϕ is the azimuthal angle, the transport equation is :

$$0 = -u\,\lambda_T(E)\cdot\frac{\partial\psi(E,u,x)}{\partial x} - \psi(E,u,x) + \int_{-1}^{1}\frac{\lambda_T(E)}{\lambda_e(E)}\cdot F_{el}(u,u')\,\psi(E,u,x)\,du' \qquad (30)$$

$$+\frac{1}{\pi}\int_{E_m}^{E_o}\int_{o}^{\pi}\frac{\lambda_T(E')}{\lambda_{inT}(E')}\cdot\mathrm{tg}^2\alpha_m\cdot\frac{E'}{(E'-E)^2}\cdot dE'.d\phi$$

with $E_m = E/\cos^2\alpha_m$.
Therefore, the use of this model needs only a knowledge of elastic m.f.p. together with either the inelastic m.f.p. or the energy losses per unit path length.

Model III - In this model, the inelastic processes are analysed in a more detailed way. In the case of aluminium, we will consider interactions with inner shell electrons, individual interactions with conduction electrons, and collective interactions with the electron gas which leads to bulk plasmon creation (87). In the case of copper, the latter two processes will be considered as a whole.

Interactions with inner shell electrons

Such interactions are the main mechanism responsible for the energy losses of charged particles. In spite of their low occurrence probability these interactions are the most important in the slowing down of the primary beam. Among the numerous analysis of the corresponding cross sections (16,28,35,65,66,90,104) we will retain those of Gryzinski (39,40,41) who uses the Coulomb collision model for two moving particles, which applies in an extended energy range, to a wide variety of materials, and to all the inner shells. In such a formulation, the differential cross section for an energy transfer ΔE from an electron with an energy E to an inner shell electron is given by :

$$\sigma(\Delta E,E,U_i) = \frac{\sigma_o}{(\Delta E)^3}\, g_\sigma\left(\frac{U_i}{E},\frac{E}{\Delta E}\right) \qquad (31)$$

with $\sigma_o = 6{,}56\ (eV)^2\ (nm)^2$, energies being expressed in eV, U_i identified with the binding energy of an "i" shell electron.

Setting : $X = \frac{E}{U_i}$ and $Y = \frac{\Delta E}{U_i}$, g_σ can be written :

$$g_\sigma(X,Y) = \frac{1}{X}\left(\frac{X}{1+X}\right)^{3/2}\left\{Y\left(1-\frac{1}{X}\right) + \frac{4}{3}\,\mathrm{Log}\left[2.718+(X-Y)^{1/2}\right]\right\}\left(1-\frac{Y}{X}\right)^{1/(1+Y)} \qquad (32)$$

The total cross section is obtained by integration over all the energy losses ; however Gryzinski gives a simple expression of the total cross section :

$$\sigma_i(E) = \frac{\sigma_o}{U_i^2}\, .\, Q(X) \qquad (33)$$

$$Q(X) = \frac{1}{X}\left(\frac{X-1}{X+1}\right)^{3/2} .\ 1+\frac{2}{3}\left(1-\frac{1}{2X}\right) .\ \mathrm{Log}\left[2.718+(X-1)^{3/2}\right] \qquad (34)$$

To take into account the angular dispersion of the incident electrons, we assume the target electron at rest. This leads to :

$$\Delta E = E\,\sin^2\alpha_m \quad 0<\alpha<\pi/2 \qquad (35)$$

where ΔE is the energy loss, E, the incident electron energy, and α, the scattering angle.

Interaction with Jellium

The dielectric theory for an infinite electron gas leads to the differential cross section for an electron of energy E, yielding an energy $\hbar\omega$, with a scattering angle α (10) :

$$\frac{d^2\sigma}{d(\hbar\omega)d\Omega} = \frac{m}{n^2\pi^2\hbar^2 a_o}\left(\frac{E-\hbar}{E}\right)^{1/2} .\ \frac{1}{q^2} .\ \mathrm{Im}\left(\frac{-1}{\varepsilon(\vec{q},\omega)}\right) \qquad (36)$$

where n is the electron number per unit volume, m the electron mass, a_o, the Bohr radius, q the momentum transfer, and $\varepsilon(\vec{q},\omega)$ the longitudinal dielectric function.

Thus, after integration on the azimuth of the scattering angle, we obtain an expression for the m.f.p. :

$$\lambda_j^{-1}(E) = \frac{2m}{\pi\hbar^2 a_o}\int_{\hbar\omega}\int_{\alpha}\left[\frac{E-\hbar\omega}{E}\right]^{1/2}\frac{1}{q^2} \cdot \mathrm{Im}\left[-\frac{1}{\varepsilon(q,\omega,\tau)}\right]\sin\alpha\, d\alpha\, d\hbar\omega \qquad (37)$$

This general formulation is convenient both for individual and collective excitations, according to the integration ranges. The dielectric loss function $\mathrm{Im}[-1/\varepsilon(\vec{q},\omega)]$ will be a theoretical or an experimental one, depending on the target material. So, in the case of aluminium, we know a theoretical loss function, and we will consider separately individual and collective interactions, while in the case of copper, we know only an experimental dielectric loss function, and we will not be able to do this separation.

Case of aluminium - The Mermin (67) dielectric function takes into account a finite lifetime of elementary excitations and can be expressed by :

$$\varepsilon(q,\omega,\tau) = 1 + \frac{(1+\frac{i}{\tau\omega})\left[\varepsilon_L(q,\omega+\frac{i}{\tau})-1\right]}{1+\frac{i}{\tau\omega}\,\frac{\varepsilon_L(q,\omega+\frac{i}{\tau})-1}{\varepsilon_L(q,o)-1}} \qquad (38)$$

where ε_L is the Lindhard's (62) dielectric function modified by introducing the complex frequency $(\omega+\frac{i}{\tau})$ and τ, the finite lifetime of the elementary excitation. τ is correlated with the damping factor γ, by the relation :

$$\gamma = \frac{1}{\tau\omega_{pl}} = \lim_{q\to o}\frac{\Delta E_{1/2}(q)}{\hbar\omega_{pl}(q)} \qquad (39)$$

ω_{pl} is the plasmon frequency, and $\Delta E_{1/2}$ is the full width at half maximum (f.w.h.m.) of the plasmon peak.
The factor γ allows us to take into account in an approximate way the dissipative processes, such as phonon losses or interactions with defects or impurities existing in a real material.
We maintain for Mermin's dielectric function the separation into two domains as is usually done with Lindhard's dielectric function. In such a way

the two interaction processes, individual and collective will be separated, even if this separation is not entirely justified with Mermin's dielectric function. For collective interaction, taking the value 15.8 eV for the energy loss by plasmon excitation in Al, and considering the dispersion of losses, we restricted the integration range to energy losses between 8 and 36 eV. The scattering angle α varies from 0 to α_c, the cut-off value which depends on the energy loss.

We have :

$$\cos \alpha_c = \frac{\left[\frac{E}{E_F} - 4y - 1 + (1+4y)^{1/2}\right] E_F}{E(1-4y\,\frac{E_F}{E})^{1/2}} \qquad (40)$$

where $y = \frac{\hbar\omega}{4E_F}$ and E is the incident electron energy.

The electron - electron scattering m.f.p. is computed by integration of relation (36) in the range $0 < E < E - E_F$ and $\alpha_c < \alpha < \alpha_{max}$ with :

$$\cos \alpha_{max} = \frac{\left[\frac{E}{E_F} - 4y - 1 - (1+4y)^{1/2}\right] E_F}{E(1-4y\,\frac{E_F}{E})^{1/2}} \qquad (41)$$

Case of copper - For the noble metals, the "d" electrons can participate in conduction phenomena. The jellium must be redefined (17) and the dielectric theory cannot be applied here. A complete theoretical calculation of the dielectric function does not exist, therefore, we used an experimental function deduced from transmission energy loss measurements carried out along the axis normal to the surface (105). Corrections must be made to eliminate the effects of multiple losses, and of surface interactions (31,78,105). The values of $\varepsilon(0,\omega)$ are thus obtained. Following the conclusions of Nagel and Witten (70), and bearing on the weak q dependence of the loss function, Ganachaud (35) proposed a separable form for $\varepsilon(q,\omega)$:

$$\varepsilon(q,\omega) = (1 + aq)\ \varepsilon(0,\omega) \qquad (42)$$

where a is a constant parameter, $\varepsilon(q,\omega)$ is the mean value of $\varepsilon(\vec{q},\omega)$ around the q direction. In the limiting case, when $q \sim 0$, both longitudinal and transverse dielectric constants can be considered to have the same value. This justifies the use of the experimentally obtained optical constant, for the dielectric constant (5,76). We can see on figure 2, that the Wehenkel's (105) loss function is very close to that of Feldkamp et al. (31) determined in the same experimental way. The most pronounced peak corresponding to a 20 eV energy loss, can be assigned to collective excitations. The fair agreement between these authors allows us to use such experimental dielectric loss function to overcome the lack of purely theoretical results. However, collective excitations do not appear clearly in the ε_1 and ε_2 curves calculated from the loss functions. Under the assumption proposed by Ganachaud (35), the loss function can be written :

$$\mathrm{Im}\left[-\frac{1}{\varepsilon(\vec{q},\omega)}\right] = \frac{1}{1+aq}\ \mathrm{Im}\left[-\frac{1}{\varepsilon(0,\omega)}\right] \qquad (43)$$

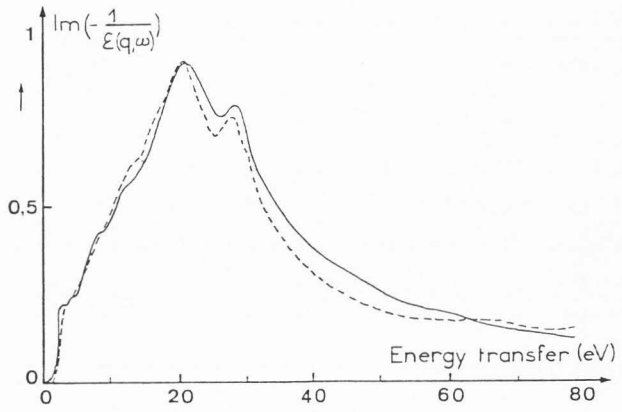

Figure 2. Dielectric loss function for copper. Full curve after Wehenkel (105), Dashed curve after Feldkamp et al. (31).

Using this relation, in the expression of λ^{-1} integration over the solid angle can be done analytically, and the inverse m.f.p. is expressed by :

$$\lambda_j^{-1}(E) = \frac{1}{\pi a_0} \int \frac{1}{E}\ \mathrm{Im}\left[-\frac{1}{\varepsilon(0,\omega)}\right] \cdot \mathrm{Log}\ \frac{\sqrt{E}+\sqrt{E'} + \frac{a}{\hbar}\sqrt{2m}\ (E-E')}{\sqrt{E}-\sqrt{E'} + \frac{a}{\hbar}\sqrt{2m}\ (E-E')}\ d(\hbar\omega) \qquad (44)$$

Concerning the angular aspect of such interactions the incoming electron suffers, generally, only small deviations. The differential cross section (36) strongly favours the small angle scattering. Probability for an angle greater than 2° is 1 % of that without deviation (Fig. 3). Thus, generally we neglect the angular deviations for such interactions.

Results for aluminium

Scattering parameters - We mention in table 1 the values of the inelastic m.f.p. used in the different models. In model II, the values are obtained from Penn (73) and Ashley (4). For model III, we give our theoretical values computed with a value $\gamma = 0.1$ for the damping factor. The values of the total inelastic m.f.p. are to be compared with those previously mentioned, and with those recently given by Penn (74). One can see that our values are close to the more recent ones. In table 2, we give the theoretical values of the energy losses per unit path length, obtained from our computations. These values, close to those of Ashley (4), are to be compared with the experimental values of Rostaing et al. (83), Lanteri et al. (58) and Fitting (32) shown in table 3. One can see, that the theoretical values are well in the range of the experimental ones, and more precisely between the values deduced from maximal range, and maximal practical range ($\eta_T < 1$ %). Thus, we use the value $\gamma = 0.1$ in our computations. The elastic m.f.p. values are mentioned in table 4, they are computed bu the "partial wave" method from data given by Ganachaud (35), and are compared with values deduced from the results of

Shimizu et al. (88). In model III, these values are used directly, while in models I and II, we used Rutherford's cross sections with a screening parameter ξ adjusted to retrieve values of the m.f.p. given in table 4. Thus, the angular dispersion is different in models I and II, from that in model III, as shown in figure 4.

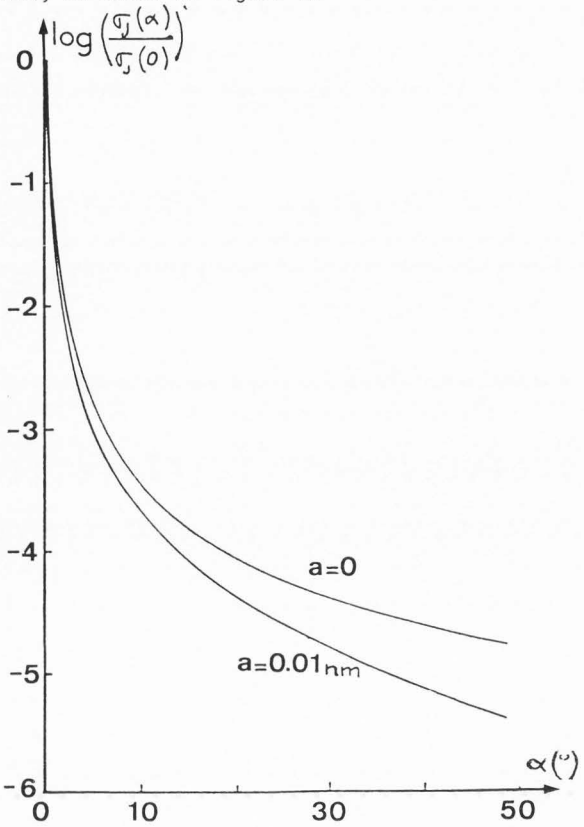

Figure 3. Angular dependence of the differential cross section for interactions with the jellium in copper.

Results - Very few experimental and theoretical results in the energy range considered here ($E_0 < 3$ keV), are available. The values of the backscattering factor η_{R0} for bulk metal, are given in table 5, as a function of the energy of the incident electrons. They are in good agreement with the experimental results of Roptin (79), Bronshtein and Fraiman (12), Thomas and Pattinson (98).

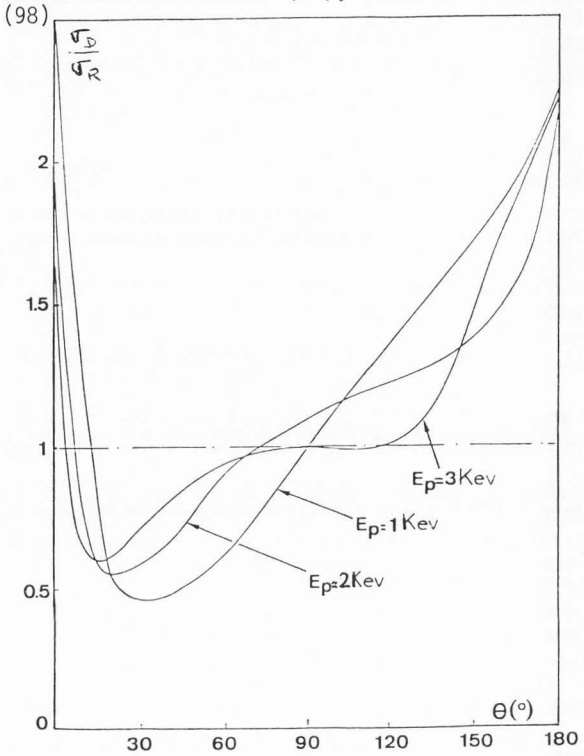

Figure 4. Ratio of the differential cross section given by the "partial wave" method, σ_D, to the Rutherford's differential cross section as function of the scattering angles for E_p = 1 keV, 2 keV and 3 keV in aluminium (from (10)).

E(keV)	3	2.5	2	1.5	1	0.5	Ref.
λ_{inT} Model II	4.7	4.12	3.5	2.8	2.07	1.22	(4) (73)
$\lambda_{e^-,pl}$	8.16	7.04	5.9	4.7	3.44	2.08	
λ_{e^-,e^-}	24.7	20.6	16.9	12.4	8.3	4.2	
λ_{L1}	215	187	159	130	103	83	our results
λ_{L23}	41	35.5	29.5	23.7	17.8	12.2	
λ_{inT} Model III	5.38	4.46	3.7	2.91	2.1	1.23	
λ_{inT}	5.2	–	3.72	2.94	2.14	1.27	(74)

Table 1. Inelastic scattering mean free paths in Al (nm). Computations of $\lambda_{e^-,pl}$ and λ_{e^-,e^-} were carried out with $\gamma = 0.1$ (λ_{inT} is the total inelastic m.f.p.).

E(keV)	3	2.5	2	1.5	1	0.5	Ref.
e^-, e^-	2.4	2.8	3.4	4.3	5.9	10.2	our
e^-, pl	2.05	2.38	2.85	3.6	4.9	8.2	results
L_1	1.36	1.51	1.71	1.97	2.27	2.35	
L_{23}	4.8	5.4	6.25	7.43	9.16	11.4	(82)
Total	10.61	12.09	14.21	17.3	22.23	32.15	
Total	11	12.7	15	18	23.4	33	(4)

Table 2. Theoretical energy losses per unit path length in Al. Computations for e^-, e^- and e^-, pl scattering were carried out with γ = 0.1 (eV/nm).

E(keV)	3	2.5	2	1.5	1	0.5	Ref.
(a)	11	12	13.5	15.7	19.5	28.1	our results
(b)	14	15.3	17.2	20	24.5	34.9	(56)
(c)	13.8	14.6	15.6	17	19.2	23.6	(32)

Table 3. Experimental energy losses in Al, eV/nm. a) from maximal range values ; b) from maximal practical range values ; c) from results of Fitting.

E(keV)	3	2.5	2	1.5	1	0.5	Ref.
λ_e (nm)	3	2.8	2.4	1.95	1.4	0.9	(88)
λ_e (nm)	2.65	2.45	2.17	1.85	1.4	0.92	(35)

Table 4. Elastic scattering mean free paths in Al (nm).

E(keV)	3	2	1.5	1	0.5	Ref.
Model I (a)	–	0.16	0.17	0.17	0.17	
Model I (b)	0.13	0.14	0.14	0.14	0.12	our results
Model II	0.21	–	0.18	0.155	0.09	(56) (58)
Model III	–	–	0.17	–	–	(82)
Extreme exp. values quoted by Kotera et al.	0.18 - 0.24	0.2 - 0.28	–	0.22 - 0.34	–	(53)
After Roptin	–	–	0.19	0.19	0.21	(79)

Table 5. Backscattering factor η_{Ro} for bulk Aluminium. a) using a maximal range ; b) using a maximal practical range. In Model II, α_m is adjusted to energy losses deduced from a maximal practical range.

The theoretical values given by Kotera et al. (53) are slightly greater than all the other values. In the case of thin targets, we show in figures 5 and 6 the theoretical variations of η_R and η_T as functions of the target thickness d, for a primary energy of 3 keV.

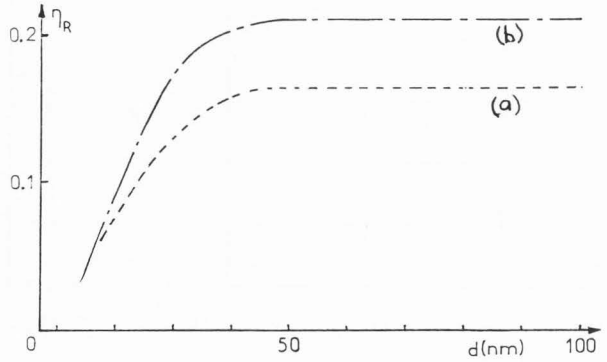

Figure 5. Backscattering coefficient η_R given by the 3 models as function of the Al target thickness d, for E_0 = 3 keV : a) Model I ; b) Models II and III.

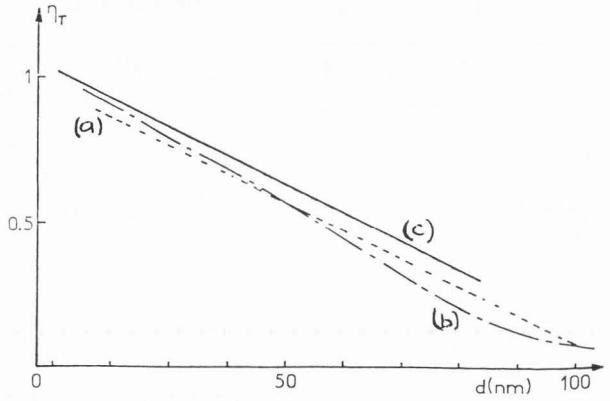

Figure 6. Transmission coefficient η_T given by the 3 models as function of the Al target thickness d, for E_0 = 3 keV : a) Model 1 ; b) Model II ; c) Model III.

The values of $\eta_T(d)$ are very close for the three theoretical models, and are in good agreement with the experimental ones. The theoretical values of $\eta_R(d)$ given by models II and III, are greater than those obtained from model I. This can be explained by the taking into account of the inelastic scattering, either in a global form (Model II) or in a detailed form (Model III). The energy distribution of electrons backscattered by the bulk metal are shown in figure 7 for E_0 = 1.5 keV. One can observe on the curve of model III the bulk plasmon losses which is the result of the use of the dielectric loss function in the computation of the diffusion function. We also show in this figure the energy distribution curve obtained by Shimizu et al. (89). These authors indicated that a more detailed analysis in the range of the characteristic energy losses reveals the existence of 6 plasmon peaks. This result is in fair agreement with the results of our computations given in a previous paper (59).

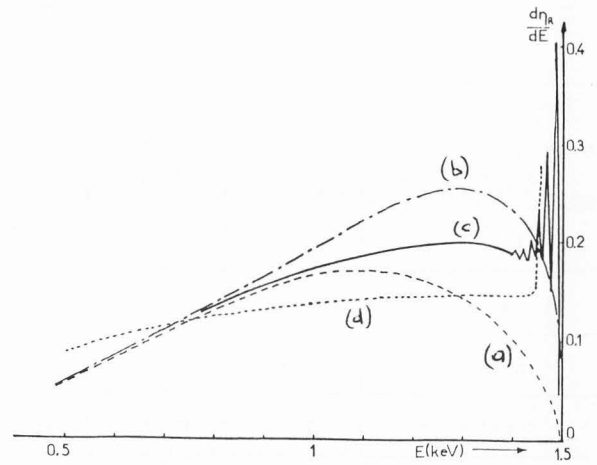

Figure 7. Energy spectra of electrons backscattered by bulk Al targets for E_0 = 1.5 keV: a) Model I; b) Model II; c) Model III; d) results of Shimizu and Ichimura (89).

The energy distributions of electrons transmitted through thin self supporting films are given for two typical cases in figures 8 and 9. In figure 8 corresponding to a 20 nm thick target, and to E_0 = 2 keV, we can observe for model III, the existence of bulk plasmon peaks. The general aspect of the curve is close to that given by model II, while the continuous slowing down model (Model I) fails. One can see in figure 9, for a 50 nm thick target, and E_0 = 3 keV, that energy distribution curves are much smoother and that bulk plasmon peaks are not very important.

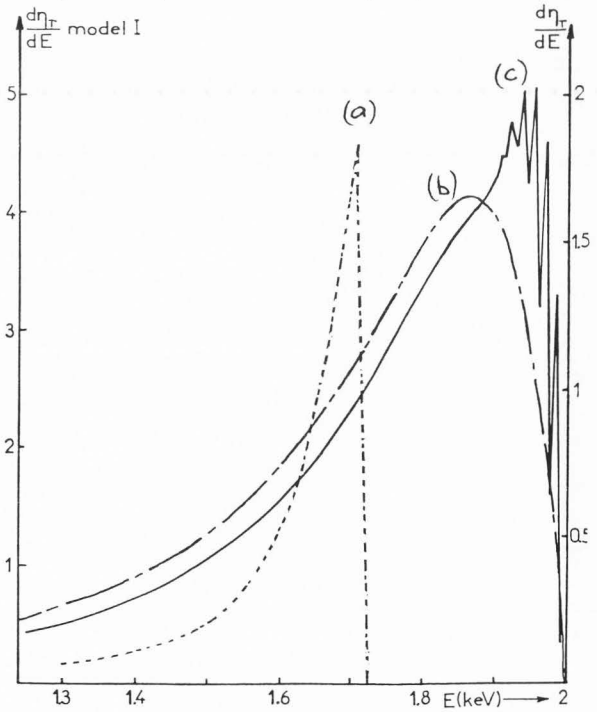

Figure 8. Energy spectra of electrons transmitted through 20 nm thick Al targets for E_0 = 2 keV : a) Model I ; b) Model II ; c) Model III.

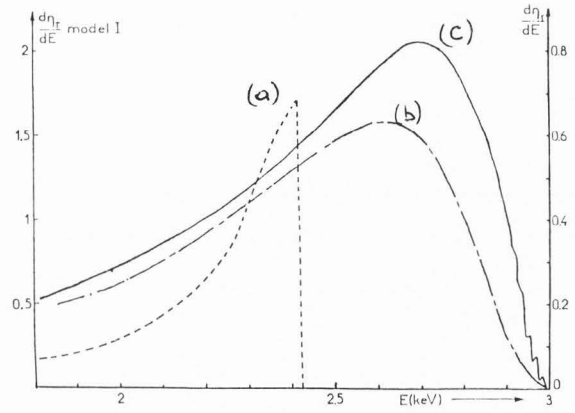

Figure 9. Energy spectra of electrons transmitted through 50 nm thick Al targets for E_0 = 3 keV : a) Model I ; b) Model II ; c) Model III.

This is the indication of a quasi complete diffusion state inside the material. These results can be compared with the experimental results of Ishigure et al. (46) and with the theoretical curves of Dejardin et al. (22). These last authors used a direct Monte Carlo simulation method, and their results are given only for primary energies lower than 1 keV, i.e., in the case of small thicknesses. We show in figures 10 and 11 the energy spectra of 1 keV incident electrons transmitted through 8 nm and 12 nm thick targets, respectively. One can see that a good agreement exists with our theoretical results. The comparison with experimental results of Ishigure et al. (46) is more difficult, due to the fact that these authors used

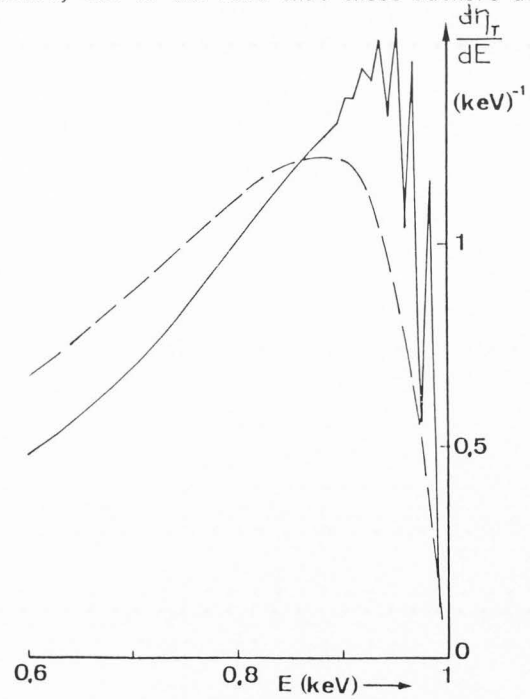

Figure 10. Energy spectra of electrons transmitted through 12 nm thick Al targets , for E_0 = 1 keV. Full curve : Model III ; dashed curve : results of Dejardin et al. (22).

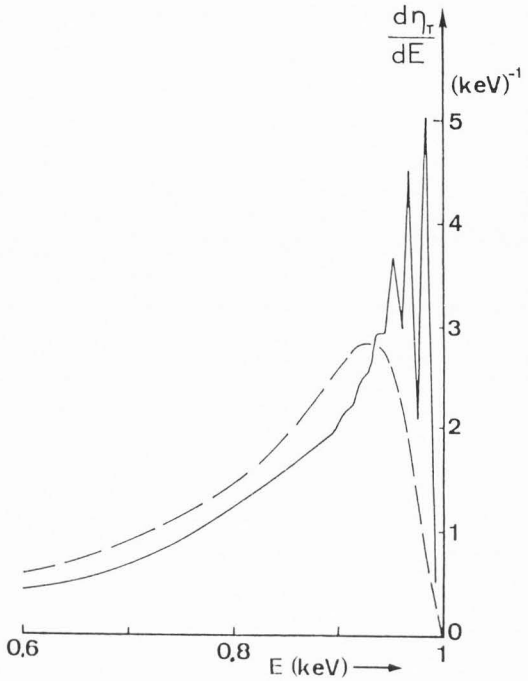

Figure 11. Energy spectra of electrons transmitted through 8 nm thick Al targets, for E_p = 1 keV. Full curve : Model III ; dashed curve : results of Dejardin et al. (22).

a 127° electrostatic velocity analyser, so that, their measurements are given in a certain number of directions, but not in the whole half space. A good agreement with our results seems however obtained with their results in a direction of emergence about 23°.

Results concerning copper

Scattering parameters. We mentioned in table 6, the values of the elastic scattering m.f.p. In model II, we used total inelastic m.f.p. values given by Cailler et al. (19), while the values of m.f.p. for all the specific processes were computed by ourselves and used in model III. The total m.f.p. values computed in this way are lower than those of Penn (74). Our computed values of energy losses per unit path length are indicated in table 7, these values are slightly lower than those of Tung et al. (101). Table 8 shows the values of energy losses per unit path length deduced from experimental range energy laws ; these values are in good agreement with the theoretical ones. As in the case of Al, the values of the energy losses given by our computations, are situated between values given by a maximal range, and a maximal practical range. The experimental values of energy losses per unit path length were used in model I. The values of the elastic m.f.p. given in table 9 were computed by the partial wave method, and were used with the corresponding cross section in model III. In models I and II, we used the Rutherford's cross section, in which the screening parameter ξ is adjusted according to the m.f.p. values of table 9.

E(keV)	3	2.5	2	1.5	1	0.5	Ref.
λ_{inT} (Model II)	2.92	2.53	2.12	1.68	1.22	0.7	(59)
λ_j a = 0.1	3.56	3.04	2.51	1.97	1.4	0.8	
λ_{M1}	161	140.5	120	100	80.6	68.6	our results
λ_{M23}	30	25.5	21.5	17.5	13.3	9.4	(83)
λ_{inT}	3.12	2.66	2.2	1.74	1.25	0.73	
λ_{inT}	4.08	-	2.95	2.35	1.73	1.07	(75)

Table 6. Inelastic scattering m.f.p. in Cu (nm). Computations of λ_j were carried out with a = 0.1. (λ_{inT} is the total inelastic m.f.p.).

E(keV)	3	2	1	Ref.
Jelium a = 0.1	22	12.4	8.8	(82)
M_{23} Shell	12.2	8.5	6.5	
M_1 Shell	2.9	2.3	1.8	
Total	37.1	23.2	17.1	
Total	50	39	30	(101)

Table 7. Theoretical energy losses per unit path length in Cu (eV/nm). Computations for scattering with Jellium were carried out with a = 0.1.

Results. Values of the backscattering factor η_{Ro} of bulk copper, for the three models, were mentioned in table 10 together with the experimental results of Pillon (75), Bronshtein (12), and Lanteri et al. (55). Whichever model is used, the theoretical results are always lower than the experimental ones. It is to be noted that values given by model II, were obtained with an adjustment of the angular dispersion of Rutherford's cross section, by means of the screening parameter ξ. Model III, in which we used a more realistic cross section computed by the partial waves method, does not allow us to obtain better results. This seems to indicate that the elastic cross section at a small angle is much more pronounced. The energy distributions of backscattered electrons by bulk copper are shown in figure 12 for all the models with E_0 = 1.5 keV. One can see that the curve given by model III shows fine structure in the neigbourhood of the primary energy. This structure reflects the peak shown by the dielectric loss function for an energy transfer of about 25 eV (fig. 2). The hump in the energy distribution curve, at approximately 80 eV, is probably due to the contribution of the M_{23} shell. This structure is also clearly apparent in figure 13 which corresponds to the backscattering by bulk copper, with E_0 = 3 keV. Concerning the general behaviour of the energy distribution curves,

E(keV)	3	2.5	2	1.5	1	0.5	Ref.
(a)	14.9	17.1	20.3	25	35	59	our results
(b)	20.7	23.9	28.4	35.5	49	84	(56) (83)
(c)	35.4	37.5	40	43.2	49	60.6	(32)

Table 8. Experimental energy losses in Cu eV/nm.

E(keV)	3	2.5	2	1.5	1	0.5	Ref.
λ_e (nm)	1.2	1.1	1	1	0.88	0.735	(35)

Table 9. Elastic scattering m.f.p. in Cu (nm).

E(keV)	3	2.5	2	1.5	1	0.5	Ref.
Model I	0.125	–	0.11	0.1	0.09	0.05	our results
Model II	0.23	–	0.22	0.22	0.205	0.15	(56) (58)
Model III	0.16	0.16	0.16	0.17	–	–	(82)
Extreme exp. values in lit.	–	–	–	0.3 - 0.37	0.3 - 0.38	0.32 - 0.36	(13) (56) (75)

Table 10. Backscattering factor η_{Ro} for bulk copper.

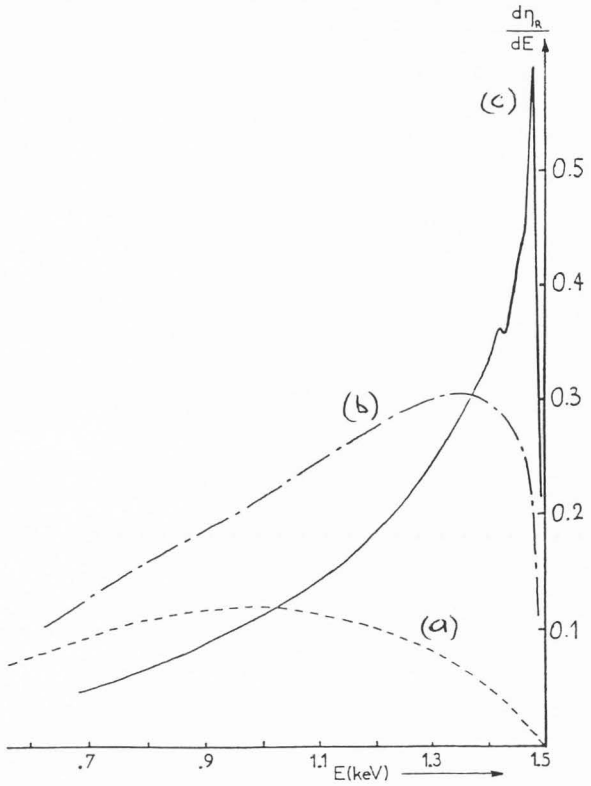

Figure 12. Energy spectra of electrons backscattered by bulk copper target, for E_0 = 1.5 keV : a) Model I ; b) Model II ; c) Model III.

one can see on figure 12 that the curve given by model I is much depressed in comparison with the others, while that given by model II, modified by the effect of the screening parameter, is close to the curve given by model III. In the case of thin self supporting targets, we presented in figures 14 and 15, the variation of the backscattering (η_R) and transmission (η_T) coefficients, with the target thickness, for E_0 = 3 keV. For $\eta_R(d)$, an asymptotic value is reached for d = 30 nm, while $\eta_T(d)$ is continuously decreasing. The values given by model II, with the screening parameter adjusted are greater than the other theoretical values. The energy distributions of 3 keV incident electrons transmitted through a 20 nm thick target, are given in figure 16. We indicated on the same figure, the

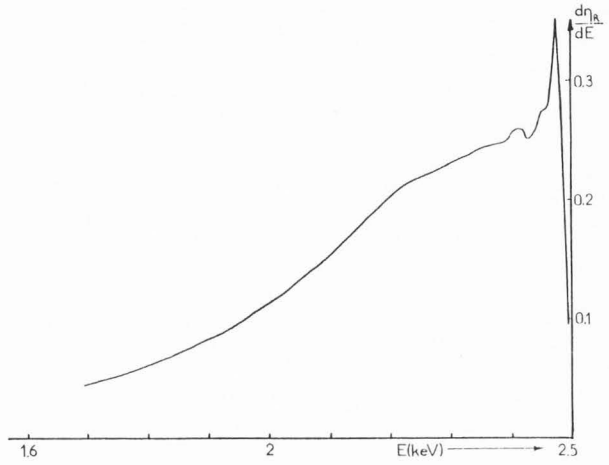

Figure 13. Theoretical energy spectrum of electrons backscattered by bulk copper target, for E_0 = 2.5 keV.

results obtained from model II, when the parameter α_m in the inelastic cross section is adjusted according to the energy losses, or to the m.f.p. values. One can see that the agreement between the two models is correct, but one must also have in mind, that in model II the directional dependence of the elastic cross section has been modified to obtain an angular behaviour, similar to the partial wave cross section. No fine structure appears on these curves, probably an indication that a complete diffusion state is reached inside the material. However, one can see in figure 17 obtained for 10 nm thick targets, that a fine structure similar to that observed by reflection, appears clearly when E_0 > 2 keV. The influence of the elastic cross section was carefully analysed by Rostaing (82) who showed that the Rutherford cross section leads to an increase of backscattering, and to a decrease of transmission. Thus, it seems that in the case of copper, an important point is the perfect knowledge of the elastic cross section. A high collision rate, together with non negligible scattering angles, leads to an angular effect of such scattering process, that are dominant compared with the other processes. The relative magnitude between transmitted and backscattered electrons is always connected to a variation of the absorption. We believe that the excessive absorption observed, is due to an

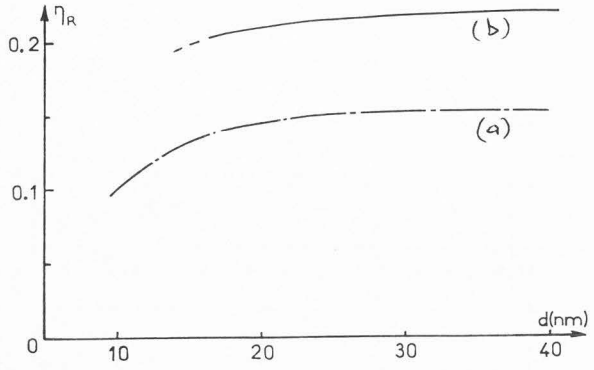

Figure 14. Backscattering coefficient η_R given by our models as function of the Cu target thickness d, for E_0 = 3 keV : a) Model II ; b) Model III.

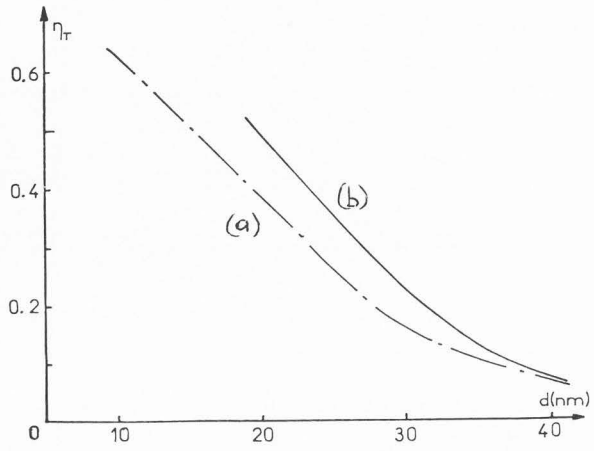

Figure 15. Transmission coefficient η_T given by our models, as function of the Cu target thickness d, for E_0 = 3 keV : a) Model II ; b) Model III.

insufficient knowledge of the elastic cross sections, leading to a less satisfactory description of the competition between the elastic scattering and the energy loss in inelastic collisions. For interactions with jellium, the assumption retained in model III, i.e., "interaction without deviation", leads to a decrease in backscattering effect. However, the contribution of such interactions to the angular dispersion, can only be of secondary importance, and cannot by itself explain the discrepancy with experimental results.

Conclusion

We showed the feasibility to build up theoretical models for electron scattering in materials, based on Boltzmann transport equation, in which, elastic and inelastic processes are described in the same way as that in Monte Carlo simulation models. Comparisons of these two types of models, when possible, give good agreement. In the case of aluminium, the three models presented here, lead for η_T to very close results. The values of η_R are identical for models II and III while model I slightly underestimate these results. Energy distribution of backscattered electrons given by the three models have the same general behaviour, while the true values given by model I are slightly too low. This model fails absolutely for the energy distribution of transmitted electrons. The advantage of model I (continuous slowing down approximation) or of the model II, in which, the energetic dispersion of inelastic processes is introduced in an approximate way, is that they can apply to a wide variety of materials. The main parameters required are in such cases : the stopping power, the total inelastic m.f.p., and the elastic m.f.p. These data can be obtained experimentally or theoretically with adjustable parameters. Thus models I and II could be used for backscattered energy distributions with or without corrections of their amplitude.

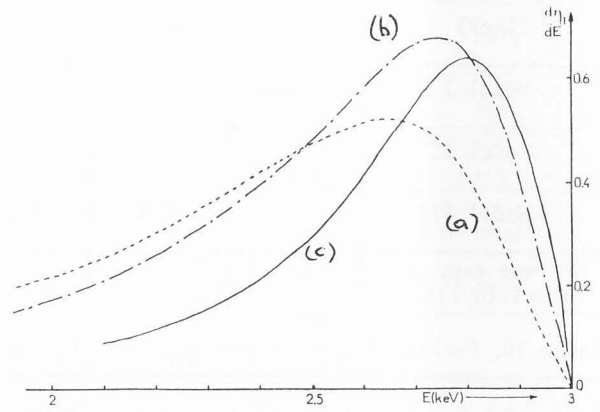

Figure 16. Energy spectra of electrons transmitted through 20 nm thick copper target, for E_0 = 3 keV : a) Model III ; b) Model II with α_m determined according to dE/dS ; c) Model II with α_m determined according to λ_{inT}.

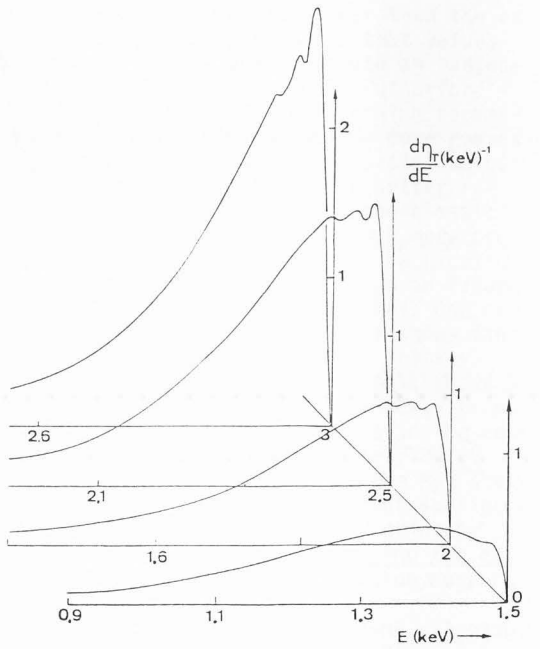

Figure 17. Energy spectra of electrons transmitted through 10 nm thick copper targets for various energies of the incident electrons.

To the contrary, model III allows the analysis of the different elementary processes. In this case, one only needs to know the values of the differential and total cross sections for all the elementary processes. These theoretical data exist only for a limited number of materials. This model is quite convenient for the analysis of the fine structure observed in energy distributions. Besides, we showed the possibility to apply such model to noble metals, using an experimental dielectric loss function. Comparison with experimental results, in spite of their scarcity in the low energy range of incident electrons, shows that it is necessary to improve the agreement, particularly for noble metals. We think that such an improvement could be obtained with model III, using a better choice of elastic and ionisation differential cross section (24,85). Thus, the application of these models to the analysis of a wide range of phenomena induced by electron bombardment can be envisaged. As a first example, we can mention, the secondary emission, a phenomenon which can also be described by means of a transport equation (25,26, 80,81,90,91). The inclusion of the energy and angular dispersion of incident electrons in the continuous slowing down approximation (Model I), was carried out by Bindi et al. (8,9). The results thus obtained are in good agreement with those obtained by a simulation method (36,37). One can also apply these models to the study of the influence of backscattered electrons in Auger spectroscopy, then compare the results with those obtained by simulation (44,97). The results given by the transport models could also be used to deduce quantitative information on the cross sections, by means of the experimental energy spectra obtained by reflection as shown by Tougaard and Chorkendorff (100).

Acknowledgements

We are grateful to C. Paparoditis for his contribution in the translation of this paper.

Symbol Table

$f(s,u,x)$	Electron density after a path length s with direction θ and depth x
$\vec{v}$	Electron velocity ($nm.s^{-1}$)
s	Electron path (nm)
x	Depth (nm)
θ	Angle of electron direction with the inward normal ; u = cos θ
Θ	Elastic scattering angle
σ_{eT}	Total cross section for elastic scattering (nm^2)
σ_e	Differential cross section for elastic scattering
F_{el}	Elastic diffusion function
$\lambda_{e\ \theta'}$	Elastic mean free path (nm)
	Angle of electron direction before scattering ; u' = cos θ'
ϕ	Azimuthal angle
n_c	Number of scattering centers per unit volume (nm^{-3})
$\Lambda_{\vec{p}_{\vec{r}}}$	Transport mean free path (nm)
	Momentum
	Position coordinates
m	Electronic mass (g)
α,α_m	Inelastic scattering angle
E_o	Energy of the incident electrons (eV)
σ_{inT}	Inelastic total cross section (nm^2)
σ_{in}	Inelastic differential cross section
$\lambda_{in},\lambda_{inT}$	Inelastic mean free path (nm)
E_{in}	Electron energy after interaction (eV)
F	Inelastic diffusion function
$\lambda_{T_{E'}}$	Total mean free path (nm)
	Electron energy before interaction (eV)
Ω	Solid angle
$\Delta E,\Delta E_i$	Energy loss (eV)
$\overline{\Delta E}$	Mean energy loss (eV)
E_F	Fermi energy (eV)
λ_i	Mean free path for the inelastic interaction i (nm)
F_i	Partial inelastic diffusion function
S	Total energy loss per unit path length
Z	Atomic number
e	Electronic charge (C)
ξ	Screening parameter
A	Atomic weight (g)
N_A	Avogadro number
ρ	Density ($g.cm^{-3}$)
$\vec{k}$	Wave vector of the incident electron
δ_ℓ	Phase shift between the ℓ partial wave and the free spherical wave
p_ℓ	Legendre polynomial
σ_o	Constant (eV^2 nm^2)
Ui	Binding energy for the i shell (eV)
X	Reduced energy
Y	Reduced energy loss
σ_i	Inelastic cross section for interaction with the i shell (nm^2)
$\hbar\omega$	Transfer of energy (eV)
a_o	Bohr radius (0.0529 nm)
$\hbar q$	Momentum transfer
ε	Dielectric function
n	Electron number per unit volume (nm^{-3})
λ_j	Mean free path for jellium interactions
τ	Lifetime of elementary excitation (s)
γ	Damping factor
ω_{pl}	Plasmon frequency (rad/s)
α_c	Cut off value of the scattering angle (Plasmon excitation)
y	Reduced energy transfer
α_{max}	Maximum scattering angle (electron - electron scattering)
$\Delta E_{1/2}$	Full width at half maximum (f.w.h.m.)(eV)
η_T	Transmission coefficient
η_R	Backscattering factor
η_{Ro}	Backscattering factor for bulk metal
d	Thickness of the target (nm)
E_m	Minimum energy transfer during inelastic scattering (eV)
l	Energy exponent in the experimental energy range relation.

References

1. Adesida I, Shimizu R, Everhart TE. (1980). A study of electron penetration in solids using a direct Monte-Carlo approach. J. Appl. Phys. 51, n°11, 5962-5969.

2. Akkerman AF, Chernov GYa. (1980). Monte Carlo calculation of the electron transmission, reflection, and absorption in solids in the energy range up to 10 keV. Phys. Stat. Sol. b, 101, 109-116.

3. Archard GD. (1961). Backscattering of electrons. J. Appl. Phys., 32, 1505-1509.

4. Ashley JC, Tung CJ, Ritchie RH. (1979). Electron inelastic mean free paths and energy losses in solids. Surf. Sci. 81, 409-426.

5. Beaglehole D. (1965). Optical properties of copper and gold in the vacuum ultraviolet. Proc. Phys. Soc. 85, 1007-1020.

6. Bennett AJ, Roth LM. (1972). Effect of primary electron diffusion on secondary electron emission. Phys. Rev. B, 5, n°11, 4309-4324.

7. Bethe HA, Rose ME, Smith LP. (1938). The multiple scattering of electrons. Proc. Am. Phil. Soc., 78, n°4, 573-585.

8. Bindi R, Lanteri H, Rostaing P. (1980). A new approach and resolution method of the Boltzmann equation applied to secondary electron emission by reflection for polycrystalline Al. J. Phys. D - Appl. Phys., 13, 267-280.

9. Bindi R, Lanteri H, Rostaing P. (1987). Secondary electron emission induced by electron bombardment of polycrystalline metallic targets. Scanning Microscopy 1, n°4, 1475-1490.

10. Bindi R, Lanteri H, Rostaing P. (1988). Transport models of scattering processes of keV electrons in aluminium. Surf. Sci., 197, 295-316.

11. Birkhoff RD. (1958). The passage of fast electrons through matter. Handbuch d. physik 34, 53-138.

12. Bronshtein IM, Fraiman BS. (1961). Inelastic scattering of electrons and secondary electron emission from certain metals and semiconductors. Sov. Phys. Solid State, 3, n°6, 1188-1196.

13. Bronshtein IM. (1969). Secondary electron emission. Ed. Naouka, Moscow.

14. Brown DB, Ogilvie RE. (1966). An electron transport model for the prediction of X-ray production and electron backscattering in electron microanalysis. J. Appl. Phys. 37, n°12, 4429-4433.

15. Brown DB, Wittry DB, Kyser DF. (1969). Prediction of X-ray production and electron scattering in electron probe analysis using a transport equation. J. Appl. Phys. 40, 1627-1636.

16. Burgess A, Percival IC. (1968). Classical theory of atomic scattering, in Advances in atomic and molecular physics. (Eds.) Bates DR and Estermann C, 4, 109-141.

17. Cailler M. (1969). Contribution à l'étude théorique de l'émission électronique secondaire induite par bombardement électronique. Thèse d'Etat, Université de Nantes, France.

18. Cailler M, Ganachaud JP. (1980). Technique de simulation Monte-Carlo de la pénétration des électrons d'énergie de l'ordre du keV, dans une cible métallique et de l'émission secondaire induite. J. Microsc. Spectrosc. Electron., 5, 415-423.

19. Cailler M, Ganachaud JP, Bourdin JP. (1981). The mean free path of an electron in copper between two inelastic collisions. Thin solid Films, 75, 181-189.

20. Cowan JJ, Hölzl J. (1976). Secondary electron transmission using straggling theory. Thin Solid Films, 92, 355-357.

21. Dashen RF. (1964). Theory of electron backscattering. Phys. Rev., 134, n°4A, A1025-A1032.

22. Dejardin-Horgues C, Ganachaud JP, Cailler M. (1976). A simulation of transmission of 1keV electrons through thin films of Aluminium, copper and gold. J. Phys. C - Solid State Physic, 9, L633-L636.

23. Desalvo A, Parisini A, Rosa R. (1984). Monte Carlo simulation of elastic and inelastic scattering of electrons in thin films : I. Valence electron losses. J. Phys. D - Appl. Phys., 17, 2455-2471.

24. Desalvo A, Rosa R. (1987). Monte Carlo simulation of elastic and inelastic scattering of electrons in thin films : II. Core electron losses. J. Phys. D - Appl. Phys., 20, 790-795.

25. Devooght J, Dubus A, Dehaes JC. (1987). Improved age-diffusion model for low energy electron transport in solids. I. Theory. Phys. Rev. B 36, 5093-5109.

26. Dubus A, Devooght J, Dehaes JC. (1987). Improved age-diffusion model for low-energy electron transport in solids. II - Application to secondary - emission from Aluminium. Phys. Rev. B, 36, 5110-5119.

27. El Gomati LL, Prutton M. (1978). Monte Carlo calculation of the spatial resolution in a scanning Auger electron microscope. Surf. Sci., 72, 485-494.

28. Estrade G. (1977). Simulation de l'ionisation interne produite par des electrons, et de la réorganisation électronique consécutive. Thèse de Spécialité, Université de Toulouse, France.

29. Everhart TE. (1960). Simple theory concerning the reflection of electrons from solids. J. Appl. Phys., 31, n°8, 1483-1490.

30. Fathers DJ, Rez P. (1979). A transport equation theory of electron backscattering. Scanning Electron Microsc., 1979; I: 55-66.

31. Feldkamp LA, Davis LC, Stearns MB. (1977). Analysis of electron inelastic scattering data with applications to Cu. Phys. Rev. B, 15, 5535-5544.

32. Fitting HJ. (1974). Transmission energy distribution and secondary electron excitation of fast electrons in thin solid films. Phys. Stat. Solid. (a), 26, 525-535.

33. Fitting HJ, Reinhardt J. (1985). Monte Carlo simulation of keV electron scattering in solid targets. Phys. Stat. Solid. (a), 88, 245-259.

34. Gaber M, Fitting HJ. (1984). Energy depth relation of electrons in bulk targets by Monte Carlo calculations. Phys. Stat. Solid. (a), 85, 195-198.

35. Ganachaud JP. (1977). Contribution à l'étude théorique de l'émission secondaire des métaux. Thèse d'Etat, Université de Nantes, France.

36. Ganachaud JP, Cailler M. (1979). A Monte Carlo calculation of the secondary electron emission of normal metals. I. The model. Surf. Sci., 83, 498-518.

37. Ganachaud JP, Cailler M. (1979). A Monte Carlo calculation of the secondary electron emission of normal metals. II. Results for Aluminium. Surf. Sci., 83, 519-530.

38. Green AJ, Leckey RCG. (1976). Scattering of 2-20 keV in Aluminium. J. Phys. D - Appl. Phys., 9, 2123-2138.

39. Gryzinski M. (1965). Two particles collisions. I. General relations for collisions in the laboratory system. Phys. Rev., 138, 305-321.

40. Gryzinski M. (1965). Two particles collisions. II. Coulomb collisions in the laboratory system of coordinates. Phys. Rev. 138, 322-335.

41. Gryzinski M. (1965). Classical theory of atomic collisions. I. Theory of inelastic collisions. Phys. Rev., 138, 336-358.

42. Henoc J, Maurice F. (1980). Diffusion simple et multiple dans la simulation des trajectoires électroniques, application au calcul de la répartition en profondeur de l'émission X. J. Microsc. Spectrosc. Electron., 5, 347-355.

43. Iafrate GJ. (1976). Electron backscattering from solids and double layers. J. Vac. Sci. Technol., 13, n°4, 843-847.

44. Ichimura S, Aratama M, Shimizu R. (1980). Monte Carlo calculation approach to quantitative Auger electron spectroscopy. J. Appl. Phys. 51, 2853-2860.

45. Ichimura S, Shimizu R. (1981). Backscattering correction for quantitative Auger analysis. Surf. Sci. 112, 386-408.

46. Ishigure N, Mori C, Watanabe T. (1978). Electron stopping power in Aluminium in the energy region from 2 to 10.9 keV. J. Phys. Soc. Jap. 44, 973-978.

47. Jablonski A. (1978). Estimation of backscattering factor for low atomic number elements and their alloys. Surf. Sci. 74, 621-635.

48. Jablonski A. (1979). Backscattering effects in Auger electron spectroscopy. A review Surf. and Interf. Analysis, 1, 122-131.

49. Jacob H. (1973). Multiple electron scattering through a slab. Phys. Rev. A 8, 226-235.

50. Jacob H. (1974). Penetration and energy deposition of electrons in thick targets. J. Appl. Phys. 45, 467-475.

51. Kanaya K, Ono S. (1978). The energy dependence of a diffusion model for an electron probe into solid targets. J. Phys. D - Appl. Phys., 11, 1495-1508.

52. Kotera M, Murata K, Nagami K. (1981). Monte Carlo simulation of 1-10 keV electron scattering in a gold target. J. Appl. Phys. 52, 997-1003.

53. Kotera M, Murata K, Nagami K. (1981). Monte Carlo simulation of 1-10 keV electron scattering in an Aluminium target. J. Appl. Phys. 52, 7403-7408.

54. Krefting ER, Reimer L. (1973). Quantitative analysis with microprobe and secondary ion mass spectroscopy. Ed. E. Preuss (Zentralbibliotek dER K.F.A.) Julich GmbH, p. 114.

55. Langeron JP. (1979). Approche analytique de la spectrométrie Auger. J. Microsc. Spectrosc. Electron 4, 431-438.

56. Lanteri H, Bindi R, Rostaing P. (1980). Modèle théorique de la rétrodiffusion d'électrons par des cibles massives d'Aluminium, d'Argent et de Cuivre. J. Phys. D - Appl. Phys. 13, 677-692.

57. Lanteri H, Bindi R, Rostaing P. (1981). Application of splitting-up method to the numerical treatment of transport equation - Analysis of the transmission of electrons through thin self supporting metallic targets. J. Comput. Phys. 39, 22-45.

58. Lanteri H, Bindi R, Rostaing P. (1982). Modèle théorique de la transmission et de la rétrodiffusion d'électrons dans des cibles métalliques minces ou semi-infinies : application à l'aluminium, l'argent et le cuivre. Thin Solid Films, 88, 309-333.

59. Lanteri H, Rostaing P, Bindi R. (1986). II. Application à l'étude des pertes caractéristiques des électrons transmis et rétrodiffusés dans le cas de l'Aluminium. Thin Solid Films, 135, 289-299.

60. Liljequist D. (1977). A simple analysis of the transmission and backscattering of 10-30 keV electrons in solid layers. J. Phys. D - Appl. Phys., 10, 1363-1377.

61. Liljequist D. (1978). Simplified models for the Monte Carlo simulation of energy distributions of keV electrons, transmitted or backscattered in various solids. J. Phys. D - Appl. Phys., 11, 839-858.

62. Lindhard J. (1954). On the properties of a gas of charged particles. Kgl. Danske Videnskab Selskab Mat. Fys. Med., 28, 8-57.

63. Love G, Cox MGC, Scott VD. (1977). A simple Monte Carlo method for simulating electron-solid interactions and its application to electron probe microanalysis. J. Phys. D - Appl. Phys., 10, 7-23.

64. McAfee WS. (1976). Determination of energy spectra of backscattered electrons, by use of Everhart's theory. J. Appl. Phys., 47, 1179-1184.

65. McGuire EJ. (1971). K and L shell fluorescence and Auger yield in Auger electron spectroscopy. J. Phys. (Paris) C4, 32, 124-127.

66. Manson ST. (1972). Inelastic collisions of fast charged particles with atoms. Ionisation of Aluminium L shell. Phys. Rev. A, 6, 1013-1024.

67. Mermin ND. (1970). Lindhard dielectric function in the relaxation time approximation. Phys. Rev. B, 1, 2362-2363.

68. Mignot H. (1974). Extension à l'or et à l'argent d'un modèle théorique de simulation de l'émission électronique secondaire induite par bombardement électronique. Thèse de 3ème cycle, Nantes, France.

69. Muller K. (1975). How much can Auger electrons tell us about solid surfaces? Springer tracts in Modern Physics, 77, 97-124.

70. Nagel SR, Whitten TA. (1975). Local fields effects on inelastic electron scattering. Phys. Rev. B, 11, 1623-1635.

71. Niedrig H. (1982). Electron backscattering from thin films. J. Appl. Phys., 53, R15-R49.

72. Patau JP, Terrissol M, Malbert M. (1980). Simulation du ralentissement des électrons entre 100 MeV et 30 keV. J. Microsc. Spectrosc. Electron., 5, 393-406.

73. Penn DR. (1976). Electron mean free paths for free-electron like materials. Phys. Rev. B, 13, 5248-5254.

74. Penn DR. (1987). Electron mean free path calculations using a model dielectric function. Phys. Rev. B, 35, 482-486.

75. Pillon J. (1974). Etude critique d'un spectroscope Auger pour l'émission électronique secondaire. Résultats obtenus sur un cristal de Cu (111). Thèse de Docteur Ingénieur, Université de Nantes, France.

76. Pines P. (1964). Elementary excitations in solids, 200-201. W.A. Benjamin Inc. New York.

77. Pouchou JL, Pichoir F, Girard F. (1980). Application de la méthode de Monte Carlo à l'analyse X des couches minces déposées sur substrat. J. Microsc. Spectrosc. Electron., 5, 425-441.

78. Raether H. (1965). Solid state excitations by electrons. Springer Tracts Mod. Phys., 38, 84-156.

79. Roptin D. (1975). Etude expérimentale de l'émission électronique secondaire de l'Aluminium et de l'Argent. Thèse de Docteur-Ingénieur, Université de Nantes, France.

80. Rösler M, Brauer W. (1981). Theory of secondary electron emission. I. General theory for nearly free electron metals. Phys. Stat. Solidi (b), 104, 161-175.

81. Rösler M, Brauer W. (1981). Theory of secondary electron emission II - Application to Aluminium. Phys. Stat. Solidi (b), 104, 575-587.

82. Rostaing P. (1983). Modèle théorique de la diffusion d'électrons de faible énergie dans les métaux. Thèse d'Etat, Université de Nice, France.

83. Rostaing P, Bindi R, Lanteri H. (1977). Application de l'équation de transport à la transmission d'électrons à travers des couches minces d'Aluminium. J. Phys. D - Appl. Phys., 10, 1191-2001.

84. Rostaing P, Bindi R, Lanteri H. (1986). Modèle théorique pour l'analyse des différents processus de diffusion dans les métaux. Thin Solid films, 135, 277-287.

85. Salvat F, Martinez JD, Mayol R, Parellada J. (1985). A simple model for electron scattering : inelastic collisions. J. Phys. D - Appl. Phys., 18, 299-315.

86. Shimizu R, Murata K. (1971). Monte Carlo calculations of the electron sample interactions in the scanning electron microscope. J. Appl. Phys., 42, 387-394.

87. Shimizu R, Kataoka Y, Matsukawa T, Ikuta T, Murata K, Hashimoto H. (1975). Energy distribution measurements of transmitted electrons and Monte Carlo simulation for kilovolt electrons. J. Phys. D - Appl. Phys., 8, 820-828.

88. Shimizu R, Kataoka Y, Ikuta T, Koshikawa T, Hashimoto H. (1976). A Monte Carlo approach to the direct simulation of electron penetration in solids. J. Phys. D - Appl. Phys., 9, 101-114.

89. Shimizu R, Ichimura S. (1983). Direct Monte Carlo simulation of scattering processes of kV electrons in Aluminium : Comparison of theoretical N(E) spectra with experiment. Surf. Sci., 133, 250-266.

90. Schou J. (1980). Transport theory for kinetic emission of secondary electrons from solids. Phys. Rev. B, 22, 2141-2174.

91. Schou J. (1988). Secondary electron emission from solids by electron and proton bombardment. Scanning Microsc. Int., I, 607-632

92. Snyder HS, Scott WT. (1949). Multiple scattering of fast charged particles. Phys. Rev., 76, n°2, 220-225.

93. Sogard MR. (1980). Backscattered electron energy spectra for thin films from an extension of Everhart theory. J. Appl. Phys., 51, 4412-4416.

94. Spencer LV. (1955). Theory of electron penetration. Phys. Rev., 98, n°6, 1597-1615.

95. Strickland DJ, Bernstein IB. (1976). Angular properties of particle fluxes for strongly forward-peaked scattering. J. Appl. Phys., 47, 2184-2190.

96. Terrissol M, Patau JP. (1980). Simulation complete des trajectoires d'électrons de quelques dizaines de keV dans les métaux. J. Microsc. Spectrosc. Electron., 5, 383-391.

97. Tholomier M, Vicario E, Doghmane N. (1987). Simulation par la méthode de Monte Carlo de l'influence des électrons rétrodiffusés en spectrométrie d'électrons Auger - 1ère partie. J. Microsc. Spectrosc. Electron., 12, 449-460.

98. Thomas S, Pattinson EB. (1970). Range of electrons and contribution of backscattered electrons in secondary production in Aluminium. J. Phys. D - Appl. Phys., 3, 349-357.

99. Tofterup AL. (1985). Theoretical aspects of quantitative electron spectroscopy. Thesis Universität Odense.

100. Tougaard S, Chorkendorff I. (1987). Differential inelastic electron scattering cross section from experimental reflection electron energy loss spectra : Application to background removal in electron spectroscopy. Phys. Rev. B, 35, 6570-6577.

101. Tung CJ, Ashley JC, Ritchie RH. (1979). Electron inelastic mean free paths and energy losses in solids II. Surf. Sci., 81, 427-439.

102. Valkealahti S, Nieminen RM. (1984). Monte Carlo calculations of keV electrons and positrons slowing down in solids. Appl. Phys. A - Solids and Surfaces, 35, 51-60.

103. Vicario E, Escudie B. (1980). Calcul, par la méthode de Monte Carlo de la distribution spatiale de l'émission électronique rétrodiffusée. J. Microsc. Spectrosc. Electron., 5, 357-370.

104. Vriens L. (1966). Electron exchange in binary encounter collision theory. Proc. Phys. Soc., 89, 13-21.

105. Wehenkel C. (1975). Mise au point d'une nouvelle méthode d'analyse quantitative des spectres de pertes d'énergie des électrons rapides diffusés dans la direction du faisceau incident : Application à l'étude des métaux nobles. Journal de Physique (Paris), 36, 199-213.

106. Weymouth JW. (1951). Multiple scattering in a semi-infinite medium. Phys. Rev., 84, 766-775.
107. Zeller C, Ruste J. (1976). Modèle théorique de la pénétration des électrons dans la matière. Revue de Physique Appliquée (Paris), 11, 441-447.

Discussion with Reviewers

H. Seiler : Can you apply the obtained results for a calculation of the contribution of backscattered electrons on secondary electron emission ?
Authors : The values of η are obtained from our models. This procedure allows us to compute the internal secondary source function, taking the effect of backscattered electrons into account. The transport of internal secondary electrons is then described by a transport equation (text refs. 8, 9, and Bindi et al. J. Phys. D. Appl. Phys. (1980) 13, 461-470). Thus one can obtain total yield $\delta = \delta_0 + C\eta$ (1). The contribution of backscattered electrons can be obtained, if we use experimental values of the relative efficiency of backscattered and primary electrons for secondary creation. This is a semi-empirical method. A purely theoretical determination of the backscattered contribution implies, after the determination of δ and η, the computation of δ_0 (the fraction of secondary electrons created by incident electrons during their direct path through material). This computation is carried out with the following assumption: All the incident electrons move through the escape region of secondary electrons with their initial direction, only the energy loss is taken into account. This allows us to perform the computation of a source function excluding the effect of backscattered electrons. From such a source function (of the secondary electron emission) one obtains a theoretical value of δ_0, and using equations, a theoretical estimate of the contribution of the backscattered electrons (Bindi et al. J. Phys. D. Appl. Phys. (1980) 13, 2351-2361).

H. Seiler : Can you estimate the dependence of the coefficient of elastically reflected electrons on the atomic number and compare the results with the values published by Schmid et al. (Scanning Electron Microsc., 1983; II: 501-509)?
Authors : The theoretical model and the numerical resolution method used in our model do not allow a realistic and reliable analysis of the elastic peak. The initial aim of these models was an application to SEE and in such a phenomenon, the elastically reflected electrons do not intervene. The fine structure observed in the neighbourhood of primary energy, is due to energy losses by plasmon excitation.

P. Rez : Could the authors tell us something about the numerical methods used to solve the transport equation and what are the likely sources of error?
Authors : Two numerical methods were used in our models. In model I, we use a "Splitting up" method (57) which is particularly successful in solving problems where the time, appears explicitly, while in models II and III, we use a "predictor-corrector" method easily applied to stationary problems. It can be shown that if these computational methods converge, they converge toward the exact solution of the equation, if the discretisation net tends toward 0 . The error of such methods is thus uniquely connected to the refinement of the discretisation net. In the two methods, for practical use, the discretisation step for s (Model I) and for E (Models II and III) we chose taking into account the minimum characteristic energy losses for all the interactions, and checking that an evolution of these steps do not introduce noticeable modification of the results. The error is also introduced for a chosen discretisation net by the computation of integral terms. To avoid such problem, we used a Gauss integration method with an order such that the integration error is always lower than the truncation error of the computer. More refined ΔE steps were used for precise analysis of characteristic energy losses (59).
P. Rez : In my experience the ratio of total inelastic to total elastic scattering is the key parameter for determining the backscattering. Could the fact that the copper backscattering is too low be due to too much inelastic scattering as compared to elastic scattering ?
Authors : Our theoretical results on copper gives values of η_R and η_T lower than the experimental values. We show (82,84) that for the same value of λ_e , a modification of the angular aspect of the elastic cross sections leads to a variation of the absorption and to a modification of the ratio between transmitted and backscattered electrons. Thus, besides the ratio of elastic to inelastic total scattering, we think that the description of the angular effect in elastic scattering is also of great importance.
P. Rez : Does neglect of exchange in the cross section lead to any serious error ?
Authors : In the energy range used here (E_p<3 keV) the inelastic m.f.p. is practically unaffected by the exchange effect,thus one can consider such an effect of minor importance for the phenomena analysed in our models.

J. Schou : How are the prospects for extending the methods, in particular method III, up to primary energies above 3 keV ?
Authors : An extension of these models, mainly Model III, up to primary energies above 3 keV do not involve particular problems, except an expense of computing time if energy steps are maintained to values below 8 eV. Indeed, in such an energy range, differential cross sections are well understood ; this is not the case in the low energy range (< 1 keV). Moreover, with primary energies over 3 keV, the experiments can be carried out more easily than for low energy, since it is comparatively easy to prepare thicker targets with a well-determined thickness and a high degree of homogeneity.